# Notes on ecosystems stability

Onofrio Mazzarisi

July 20, 2022

## 1 Complexity-stability regimes

In this section we describe how the relationship between complexity and stability is shaped by dynamical properties of complex ecosystems. Refine this Intro

Consider a competitive community of $S$ species defined by the following dynamics for the population abundances

$$\frac{dx_i}{dt} = x_i^\alpha - x_i^\beta \sum_j A_{ij} x_j^\gamma \,, \tag{1}$$

where the sum runs from $j = 1$ to $j = S$ and the off-diagonal elements of $A$ are extracted from a distribution with mean $\mu > 0$ and standard deviation $\sigma$ while $A_{ii} = 1/K^{\beta+\gamma-\alpha}$, $\forall i$, and $K$ is the (uniform) carrying capacity. If the equilibrium is feasible it formally reads

$$(x_i^*)^{\alpha-\beta} = \sum_j A_{ij} (x_j^*)^\gamma \,. \tag{2}$$

The element of the jacobian for $j \neq i$ read

$$J_{ij} = -\gamma x_i^\beta A_{ij} x_j^\gamma \,, \tag{3}$$

while the diagonal components read

$$J_{ii} = \alpha x_i^{\alpha-1} - \beta x_i^{\beta-1} \sum_{j\neq i} A_{ij} x_j^\gamma - (\beta+\gamma) A_{ii} x_i^{\beta+\gamma} \,. \tag{4}$$

In the case of uniform interactions ($\sigma \to 0$) the species population are all equal and the equilibrium reads

$$x^* = \left[ \mu(S-1) + \frac{1}{K^{\beta+\gamma-\alpha}} \right]^{1/(\alpha-\beta-\gamma)} \,. \tag{5}$$

The jacobian evaluated at equilibrium is

$$J_{ij}\Big|_{x=x^*} = -\gamma \mu (x^*)^{\beta+\gamma-1} \,, \tag{6}$$

$$J_{ii}\Big|_{x=x^*} = \alpha (x^*)^{\alpha-1} - \beta (x^*)^{\beta+\gamma-1} \mu (S-1) - \frac{(\beta+\gamma)}{K^{\beta+\gamma-\alpha}} (x^*)^{\beta+\gamma-1} \,. \tag{7}$$

The maximum eigenvalue $\lambda_{\max}$ is $S-1$ degenerate and reads formally

$$\lambda_{\max} = J_{ii}\Big|_{x=x^*} - J_{ij}\Big|_{x=x^*} \,. \tag{8}$$

The stability condition

$$\lambda_{\max} = \alpha(x^*)^{\alpha-1} - (x^*)^{\beta+\gamma-1}\left[\beta\mu(S-1) + \frac{(\beta+\gamma)}{K^{\beta+\gamma-\alpha}} - \gamma\mu\right] < 0\,, \tag{9}$$

can be written as

$$\alpha(x^*)^{\alpha-\beta-\gamma} - \left[\beta\mu(S-1) + \frac{(\beta+\gamma)}{K^{\beta+\gamma-\alpha}} - \gamma\mu\right] < 0\,, \tag{10}$$

which, using the expression for $x^*$ and after some manipulations reads

$$(S-1)(\beta-\alpha) > \frac{K^{\beta+\gamma-\alpha}\mu\gamma + \alpha - \beta - \gamma}{K^{\beta+\gamma-\alpha}\mu}\,. \tag{11}$$

We have then three possibilities:

$$S > 1 + \frac{K^{\beta+\gamma-\alpha}\mu\gamma + \alpha - \beta - \gamma}{K^{\beta+\gamma-\alpha}\mu(\beta-\alpha)} \qquad \text{if} \quad \alpha < \beta\,, \tag{12}$$

$$S < 1 + \frac{K^{\beta+\gamma-\alpha}\mu\gamma + \alpha - \beta - \gamma}{K^{\beta+\gamma-\alpha}\mu(\beta-\alpha)} \qquad \text{if} \quad \alpha > \beta\,, \tag{13}$$

$$\mu < \frac{1}{K^\gamma} \qquad \text{if} \quad \alpha = \beta\,. \tag{14}$$

A series of comments is in order.

- Depending on $\alpha$ and $\beta$ we have *two regimes*: one in which increasing $S$ enhances stability ($\alpha < \beta$) and one in which it hinders stability ($\alpha > \beta$). Notably this is independent from $\gamma$, indicating that only the interplay between the density dependence of the contribution of a species to the interactions and the density dependence of its production term that is (qualitatively) relevant; and not the form of the contribution of the competitors to the interactions.
- The critical case ($\alpha = \beta$) recovers the usual GLV result for $\gamma = 1$ and generalizes it for generic $\gamma$.
- For $K \to \infty$ and $\beta = 1 = \gamma$ we obtain

$$S = 1 + \frac{1}{1-\alpha}\,. \tag{15}$$

For symmetry reasons, it is probably sensible to consider models with $\gamma = \beta$, leaving the potential asymmetry of the competitive interaction between two species to the coefficient $A_{ij}$.

One can therefore identify two different regimes (complexity hinders stability (May) and complexity increases stability) characterized by the dynamical response of the population with respect to their density encoded in the exponents $\alpha$ and $\beta$, resepctively associated to production and losses. The GLV case $\alpha = \beta$ is right in the middle for uniform interactions ($\sigma \to 0$) and falls into the May regime otherwise ($\sigma \neq 0$).

## 2 On sublinear production

Observations point towards sublinear production scaling with respect to the population biomass density. This observations may refer to dynamical production or to the equilibrium production observed across a biomass gradient.

In this section we discuss how, although dynamical sublinear production does not generally leads to sublinear production across a biomass gradient, it might be necessary for sublinear scaling across a biomass gradient.

Let us focus on a single population example to calrify ideas. Consider a production function of the form

$$g(x) = rx^{\alpha}\,, \tag{16}$$

where $x$ is the abundance of the population, $\alpha \leq 1$ specify the intensity of sublinear dynamical scaling (linear when $\alpha = 1$) and $r$ is the parameter that allows to move across a gradient. Consider then a loss term of the form

$$l(x) = zx^{\beta}\,. \tag{17}$$

The evolution equaiton for the population is

$$\frac{dx}{dt} = g(x) - l(x) = rx^{\alpha} - zx^{\beta}\,, \tag{18}$$

which reduces to logistic growth for $\alpha = 1$ and $\beta = 2$. The equilibrium is given by

$$x^* = \left(\frac{r}{z}\right)^{1/(\beta-\alpha)}\,, \tag{19}$$

and the stability condition is given by

$$\left.\frac{d\left[g(x) - l(x)\right]}{dx}\right|_{x=x^*} < 0\,, \tag{20}$$

which leads, after some calculations, to the condition

$$\alpha < \beta\,, \tag{21}$$

independent from $r$ and $z$.

The equilibrium production scales, at varying growth rate $r$, as $g(x^*) = z(x^*)^{\beta}$ as can be noted by Eq. (19) for $r$ and then substituting it in the defining Eq. (16) or simply by considering the dynamical equation at stationarity. Notice that, if $z$ is varied instead, the exponent of dynamical and across-gradient production coincide.

In summary, for an environmental change that amount to a change in $r$, the production across a gradient scales as $(x^*)^{\beta}$. In order for the stationary solution to be stable an exponent $\alpha < \beta$ for the dynamical produciton is needed. Therefore, in order to have sublinear $g(x^*)$ across a gradient, we need $\alpha < \beta < 1$. If the increment of the equilibrium density is due to decreasing $x$, equilibrium and dynamical production scale in the same way and in order to have sublinear $g(x^*)$ we need $\alpha < 1$ with $\alpha < \beta$ for stability but no constraint on $\beta$. Either way we need $\alpha < 1$.

## 3 Cavity solution for sublinear growth

In this section we derive the cavity solution which is used in the main text.

Let us consider the dynamics of the population abundances $x_i$ for $S$ species

$$\frac{dx_i}{dt} = r_i x_i^k - x_i \sum_{j \neq i} A_{ij} x_j\,, \tag{22}$$

where the entries of the interaction matrix $A_{ij}$ and are randomly distributed with average $\mu$ and standard deviation $\sigma$ and the $r_i$ are growth rates extracted from a distribution $P(r)$.

Cavity trick description ... (Refs. [1, 2, 3, 4, 5])

The cavity solution is the random variable $x^*$ given by

$$x^* = \left( \frac{\mu S \langle x^* \rangle + \sigma \sqrt{S \langle (x^*)^2 \rangle} \eta}{r} \right)^{1/(k-1)} , \tag{23}$$

where $\langle x^* \rangle$ and $\langle (x^*)^2 \rangle$ are the first two moments of the equilibrium average biomass density and $\eta$ is a standard normal random variable, i.e. $P(\eta) = \mathcal{N}(0,1)$. The equilibrium probability distribution function for $x^*$, $P(x^*)$, can be obtained through the pushforward of the distribution of $\eta$ and $r$ add details of derivation

$$P(x^*) = \frac{(1-k)|x^*|^{k-2}}{\sqrt{2\pi\sigma^2 S \langle (x^*)^2 \rangle}} \int_0^\infty dr \; r P(r) \exp\left\{ - \frac{\left[ (x^*)^{k-1} - \mu S \langle x^* \rangle / r \right]^2}{2\sigma^2 S \langle (x^*)^2 \rangle / r^2} \right\} , \tag{24}$$

where the fraction of survival species $\phi$ and the first two moment have to be self-consistently computed

$$\begin{aligned} \phi &= \int_0^\infty dx^* \; P(x^*) , \\ \langle x^* \rangle &= \frac{1}{\phi} \int_0^\infty dx^* \; x^* P(x^*) , \\ \langle (x^*)^2 \rangle &= \frac{1}{\phi} \int_0^\infty dx^* \; (x^*)^2 P(x^*) . \end{aligned} \tag{25}$$

In the case of a unique $r$ for every species in the community, i.e. $P(\bar{r}) = \delta(r - \bar{r})$ the distribution reads

$$P(x^*) = \frac{(1-k)|x^*|^{k-2}}{\sqrt{2\pi\sigma^2 S \langle (x^*)^2 \rangle / r^2}} \exp\left\{ - \frac{\left[ (x^*)^{k-1} - \mu S \langle x^* \rangle / r \right]^2}{2\sigma^2 S \langle (x^*)^2 \rangle / r^2} \right\} . \tag{26}$$

We can't formally solve the self-consistent equations (25) because the first and second moment of for this distribution diverges. A similiar problem is encountered in Ref. [5] in the context of consumer-resource models for the cavity calculations of the distribution of the resources which is, *mutatis mutandis*, equivalent of our case for $k = 2$. (We should take into account that the cavity solution is an idealization of the initial problem and this kind of pathologies are not necessarely realistic. For example extreme value theory [6] predicts that on average the largest value observed in a system of size $S$ scales like $S$ itself. On the other hand the distribution as $S$ increases becomes closer to a gaussian and eventually all the heterogeneity disappears because of the size dependence of the term multiplying $\eta$ is quadratic while the one multuplying $\mu$ is linear and dominates for very large $S$.)

Refine or remove these explanations.

Assuming that the fluctuations in the numerator in Eq. (23) are small, i.e. $\sigma \sqrt{S \langle (x^*)^2 \rangle} \ll \mu S \langle x^* \rangle$, we can Taylor expand to the first-order the cavity solution obtaining

$$x^* = \left( \frac{\mu S \langle x^* \rangle}{r} \right)^{1/(k-1)} - \frac{1}{1-k} \left( \frac{\mu S \langle x^* \rangle}{r} \right)^{(2-k)/(k-1)} \sigma \sqrt{S \langle (x^*)^2 \rangle} \eta , \tag{27}$$

which is a gaussian variable, truncated in 0 to respect non-negativity constraint, with mean

$$\langle x^* \rangle = \left( \frac{\mu S \langle x^* \rangle}{r} \right)^{1/(k-1)} , \tag{28}$$

and standard deviation

$$\sqrt{\langle (x^*)^2 \rangle - \langle x^* \rangle^2} = \frac{1}{1-k} \left( \frac{\mu S \langle x^* \rangle}{r} \right)^{(2-k)/(k-1)} \sigma \sqrt{S \langle (x^*)^2 \rangle} \, . \tag{29}$$

In this approximation we can solve analytically the self consistency equations for the first to moment of the distribution as functions of the parameters, namely

$$\langle x^* \rangle = \left( \frac{\mu S}{r} \right)^{1/(k-2)} , \tag{30}$$

and

$$\langle (x^*)^2 \rangle = \frac{\langle x^* \rangle^2}{\left[ 1 - \left( \frac{1}{1-k} \right)^2 \langle x^* \rangle^{2(2-k)} \sigma^2 S \right]} \, . \tag{31}$$

We can now either use directly the gaussian approximation to describe the species distribution or alternative use the moment evaluated by means of the gaussian approximation in expression

For practical purposes we can also solve numerically the self-consistent equations (25) using a large upper cut off $x_{\rm up}$ which we checked can be widely varied and gives consistent results. In Fig. 1 we report comparisons of the cavity solution (26) obtained solving numerically the self-consistent equations, the one with the moment injected from the gaussian calulation and the approximated gaussian solution.

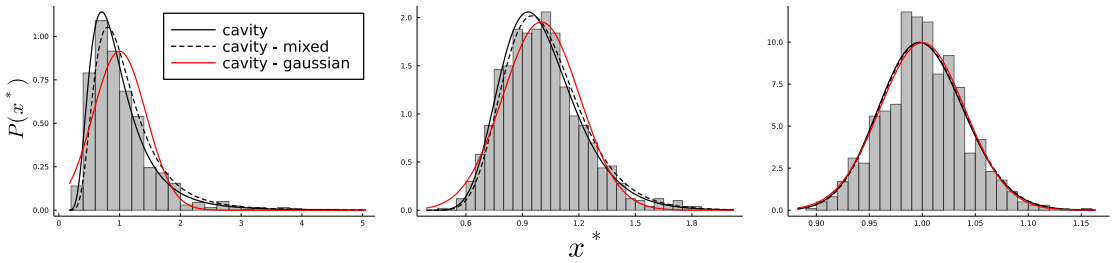


Figure 1: Cavity solution in Eq. (26) (black solid line) with the moment numerically self-consistently computed from the full distribution, the mixed approximation (black dashed line) obtained using the gaussian moments in Eq. (26) and the gaussian approximation (red line) are compared with simulation for a system of $S = 10^3$ species with $r = 1$, $\mu = 10^{-3}$, $k = 3/4$ and $\sigma = \mu/10$ (left), $\sigma = \mu/20$ (center) and $\sigma = \mu/100$ (right).

## 3.1 Dynamical mean field theory

In order to obtain information about the dynamics of the distributions of the biomass densities of the community, following, e.g., Ref. [7] we can derive from Eq. (22), for large $S$, a dynamical mean field theory which provide us a stochastic differential equation describing statistically the entire ensemble of species thorug the evolution of the represenntive random variable $x$

$$\frac{dx}{dt} = r x^k - x \left( \mu S \langle x \rangle_t + \sigma \sqrt{S} \eta_t \right) , \tag{32}$$

where $\langle x\rangle_t = \langle x(t)\rangle$ is the average at time $t$ of the random variable $b$ and $\eta$ is a gaussian variable with zero mean and correlation given by $\langle x(t)x(s)\rangle$; these first and second moment have to be computed self-consistently at each time. At equilibrium the cavity solution is recovered.

From Eq. (32) is possible to connect the arguments about sublinear growth for the one dimensional model in Section 2 to a competitive community.

Figure out if leave or not this subsection.

## 4 Boundary of stable phase in $(\mu, \sigma)$ plane

double-check a la Stone derivation of the results and finish derivation for the calculation of the critical line.

In this section we combine the results from Ahmadian *et al.* [8] on the distribution of eigenvalues in the complex plane with the cavity solution derived in Section 3 to obtain a line in the $(\mu, \sigma)$ plane separating a stable and an unstbale phase.

In Ref. [8] is shown that the spectrum of matrices of the form $M + LJR$, where $M$, $L$ and $R$ are $S \times S$ deterministic matrices and $J$ is a $S \times S$ random matrix whose coefficients have mean zero and variance $\sigma^2$ is contained in the region of the complex plane

$$\mathrm{Tr}[(M_z M_z^\dagger)^{-1}] \geq 1/\sigma^2 \quad \text{where } M_z = L^{-1}(zI - M)R^{-1}, \tag{33}$$

where Tr denotes the trace of the matrix. In the special case where $L$, $R$ and $M$ are diagonal, this condition reads

$$\sum_{i=1}^{S} \frac{(L_i R_i)^2}{|z - M_i|^2} \geq 1/\sigma^2. \tag{34}$$

Consider the system of $S$ species defined by

$$\frac{dx_i}{dt} = x_i g(x_i) - x_i \sum_{j \neq i} A_{ij} x_j \,, \tag{35}$$

where the $g(x_i)$ is the per capita growth rate and $A$ is a matrix with zero diagonal and off-diagonal elements ditrubuted with mean $\mu$ and standard deviation $\sigma$.

We can apply this result to estimate the location of the eigenvalues of the community matrix $C$, defined as the jacobian of the system evaluate equilibrium point $\mathbf{x}^*$. The off diagonal elements of the jacobian at equilibrium are

$$J_{ij}\Big|_{\mathbf{x}=\mathbf{x}^*} = -x_i^* A_{ij} \,, \tag{36}$$

while the diagonal reads

$$J_{ii}\Big|_{\mathbf{x}=\mathbf{x}^*} = -\sum_{j \neq i} A_{ij} x_j^* + g(x_i^*) - x_i^* g'(x_i^*) = -x_i^* g'(x_i^*) \,, \tag{37}$$

where for the last equality we used the equilibrium relation and $g'(x_i^*) := dg(x_i)/dx_i|_{x_i = x_i^*}$. The community matrix therefore reads

$$C = -D(\mathbf{x}^*)A - D(\mathbf{x}^* g'(\mathbf{x}^*)) \,, \tag{38}$$

where we denote $D(\mathbf{y}) := \mathrm{diag}(\mathbf{y})$ stands for a diagonal matrix filled with the components of the vector $\mathbf{y}$. Writing $A = \mu \mathbf{1} - \mu I + J$, and identifying $L = -D(\mathbf{x}^*)$, $R = I$ and $M =$

$\mu I - D(\mathbf{x}^* g'(\mathbf{x}^*))$ we can say that the eigenvalues lie within the domain

$$\sum_i \frac{(x_i^*)^2}{|z - \mu + x_i^* g'(x_i^*)|^2} \geq 1/\sigma^2. \tag{39}$$

This domain touches $z = 0$ (triggering an instability) whenever

$$\sum_i \frac{1}{|\mu - P(n_i^*)/(n_i^*)^2 + P'(n_i^*)/n_i^*|^2} \geq 1/\sigma^2 \,. \tag{40}$$

# 5 Extinction threshold

In this section we derive an expression to estimate the extinction threshold in parameter space. It can be obtained by means of the gaussian approximation of the cavity solution.

We recall the definition for the first and second moment of the distribution of $x$

$$\langle x^* \rangle = \left( \frac{\mu S}{r x_0^{1-k}} \right)^{1/(k-2)} , \tag{41}$$

and

$$\langle (x^*)^2 \rangle = \frac{\langle x^* \rangle^2}{\left[ 1 - \left( \frac{1}{1-k} \right)^2 \langle x^* \rangle^{2(2-k)} \sigma^2 S \right]} , \tag{42}$$

where we explicitely wrote down the scale $x_0$ because in the following we want to study both, the case where the growth term is not modified below threshold and when is set equal to zero causing every species below threshold to go extinct.

First we approximate the second moment by expanding it to the first order in the second addend in the denominator

$$\langle (x^*)^2 \rangle \approx \langle x^* \rangle^2 + \left( \frac{1}{1-k} \right)^2 \langle x^* \rangle^{2(3-k)} \sigma^2 S \,, \tag{43}$$

so that the standard deviation can be written as

$$\sqrt{\langle (x^*)^2 \rangle - \langle x^* \rangle^2} \equiv \mathrm{std}(x^*) = \left( \frac{1}{1-k} \right) \langle x^* \rangle^{(3-k)} \sigma \sqrt{S} \,. \tag{44}$$

Now we want to write down the condition under which the average minus a number $\nu$ of standard deviations touches zero, or $x_0$ if the threshold is enforced. Let us consider this latter more general case first. The condition reads

$$\langle x^* \rangle - \nu \ \mathrm{std}(x^*) = x_0 \,, \tag{45}$$

which, using Eq. (44), becomes

$$\langle x^* \rangle - \nu \left( \frac{1}{1-k} \right) \langle x^* \rangle^{(3-k)} \sigma \sqrt{S} = x_0 \,. \tag{46}$$

Substituting the expression for the average and solving for $\sigma\sqrt{S}$, we finally obtain

$$\sigma \sqrt{S} = \frac{1-k}{\nu} \left[ \left( \frac{\mu S}{r x_0^{1-k}} \right) - x_0 \left( \frac{\mu S}{r x_0^{1-k}} \right)^{(k-3)/(k-2)} \right] , \tag{47}$$

which reduces to the linear relation between the scaled parameters $\sigma\sqrt{S}$ and $\mu S$

$$\sigma\sqrt{S} = \left(\frac{1-k}{\nu r x_0^{1-k}}\right)\mu S\,. \tag{48}$$

In order to avoid arbitrariness in the choice of $\nu$ we can estimate an $S$ dependent value which accounts for the fact that the same equilibrium distribution but with more species (therefore the same point in the $\sigma\sqrt{S} - \mu S$ plane for higher $S$) implies a smaller sample minimum. One way to make analytical progress is to impose is to find the value $x_{\min}$ for which the gaussian approximation for the distribution touches $1/S$. Tehre will be two points satisfying this conditions and we are interested in the lower one. The rationale behind this is that in a community of $S$ species, less then one on average will be below $x_{\min}$. We have

$$\frac{1}{\sqrt{2\pi \mathrm{std}(x^*)^2}}\exp\left[-\frac{(x_{\min}-\langle x^*\rangle)^2}{2\mathrm{std}(x^*)^2}\right] = \frac{1}{S}\,, \tag{49}$$

which, solving for $x_{\min}$, gives

$$x_{\min} = \langle x^*\rangle - \mathrm{std}(x^*)\sqrt{2\ln\left(\frac{S}{\sqrt{2\pi\mathrm{std}(x^*)^2}}\right)}\,. \tag{50}$$

For large $S$ we can approximate the last equation by

$$x_{\min} = \langle x^*\rangle - \sqrt{2\ln S}\;\mathrm{std}(x^*)\,, \tag{51}$$

from which we can read our estimate for $\nu$, comparing with Eq. (45), i.e.

$$\nu = \sqrt{2\ln S}\,. \tag{52}$$

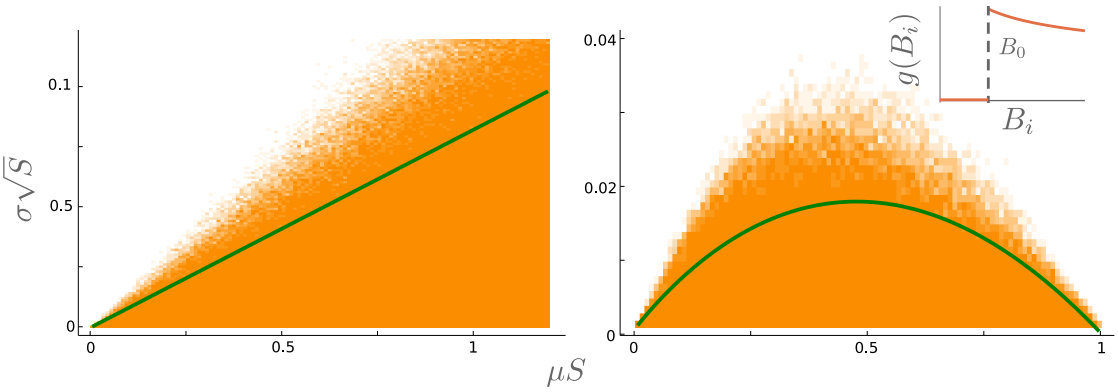


Figure 2: ...

In Fig. (2) ...

## 5.1 GLV case

The same arguments apply to GLV, which, we recall, describes $S$ species evolving as

$$\frac{dx_i}{dt} = rx_i(1-\frac{x_i}{K}) - x_i\sum_{j\neq i}A_{ij}x_j \tag{53}$$

with $A_{ij}$ distributed with mean $\mu$ and standard deviation $\sigma$ and we assume here $r$ and $K$ equal for all species, allowing to estimate the extinction threshold also in this case.

The equilibrium distribution obtained through the cavity method is a truncated gaussian [REFS] with average

$$\langle x^* \rangle = \frac{K}{1 + K\mu S/r} \,, \tag{54}$$

and standard deviation, written as a function of the average,

$$\mathrm{std}(x^*) = \frac{\sigma\sqrt{S}K\langle x^* \rangle}{\sqrt{1 - \frac{K^2\sigma^2 S}{r^2}}} \,, \tag{55}$$

plugging in the last two equations in the extinction threshold condition (45), for $x_0 = 0$ leads to

$$\sigma\sqrt{S} = \frac{r}{K\sqrt{\nu^2 + 1}} \,, \tag{56}$$

which is an horizontal line in the parameter space lower then the stability condition $\sigma\sqrt{S}$ and recovers it for $\nu = 0$.

## 6 Model connection with data on productivity

Our model is informed by macroecological observations of biomass density production across major groups. In this section we attempt a closer connection to the data.

We define our model in the following way

$$\frac{db_i}{dt} = \underbrace{r_i b_i \left(\frac{b_i}{b_0}\right)^{k-1} \theta(b_i - b_0)}_{\text{Production}} - \underbrace{b_i \sum_{j \neq i} A_{ij} b_j}_{\text{Losses}} \,, \tag{57}$$

where $k < 1$ specify the intensity of sublinear dynamical scaling, the entries of the interaction matrix $A_{ij}$ are randomly distributed with average $\mu$ and standard deviation $\sigma$, the $r_i$ are growth rates extracted from a distribution $P(r)$, the biomass density scale $b_0$. For the sake of clarity let us summarize the dimensionality of the several terms involved in the model

$$[b_i] = [b_0] = \frac{\text{mass}}{\text{area}} \,, \quad [r_i] = \frac{1}{\text{time}} \,, \quad [A_{ij}] = \frac{\text{area}}{\text{mass} \times \text{time}} \,. \tag{58}$$

The density biomass scale $b_0$ set the value at which the per capita growth rate is $r_i$. When we want to consider this value the maximum per capita growth rate for a given species we can consider $b_0$ as the minimal biomass density for a given species at which it is able to reproduce. In this case we can impose that there is no growth for $b_i < b_0$ through a Heaviside function $\theta(b_i - b_0)$.

Next we connect the model with the average body mass $m$ of a community. The time scale of the problem are widely observed [9] to scale with the body mass with an exponent $-1/4$. Therefore we assume that the average growth rate $\langle r \rangle$ for a community and the average interaction $\mu$ scale with the average body mass of the community to the $-1/4$, i.e. $\langle r \rangle \sim m^{-1/4}$ and $\langle \mu \rangle \sim m^{-1/4}$. We have no reasons to assume a systematic variation of the ratio $\mu/\sigma$ with respect to the mass. We assume for simplicity that $b_0$ is species and mass independent. We may invoke an ecological argument to justify this assumption, indeed the observed biomass densities

across major group have a mass independent lower bound (within two or three order of magnitude compared with the astronomical difference of nearly 20 order of magnitude in body mass). The population density scale for a given community of average mass $m$, $n_0 := (b_0)/m$, is then assumed to be inversely proportional to the mass.

To compare this data with outcomes of the model we proceede as follows. We characterize a community type by an average mass, and therefore by an average growth rate $\langle r \rangle$, then we solve the model for different communities with same average $r$ but different $\mu$ and plot the resulting $\langle b^* \; g(b^*) \rangle$ vs $\langle b^* \rangle$. In this process we keep the coefficient of variation $\sigma/\mu$ constant. We keep $S$ constant and vary $\mu$ in a range which scales with $m$ in the same way that the average $r$ does across community type: within a community type we plot results for communities with $\mu S \in (\langle r \rangle \mu_{\min}, \langle r \rangle \mu_{\max})$, with $\mu_{\min}$ and $\mu_{\max}$ possibly mass dependent but with $\mu_{\min} < 1$ and $\mu_{\max} > 1$. In other words, in order to not introduce strong biases towards specific masses, within community type and for every community type, we simulate different environment going from a $\mu$ which is less than $\langle r \rangle$ to one which is more than $\langle r \rangle$. We can summarize the assumptions in the following way.

**Assumptions**

- $b_0$ is body mass independent and $n_0$ for a community is inversely proportional to the average body mass $m$ of the community.
- $r \sim m^{-1/4}$ and characterize the typical growth rate of a community type with the typical body mass $m$.
- $\mu \sim m^{-1/4}$ for a given community type of average mass $m$.
- To explore ecological variation among communities of the same type we cosider different $\mu S \in (r\mu_{\min}, r\mu_{\max})$ with $\mu_{\min} < 1$ and $\mu_{\max} > 1$.
- the coefficient of variation $\mu/\sigma$ does not vary systematically both within and across community type.
- $k < 1$, in particular, in orderd to closely recover the observed pattern, $k \simeq 3/4$

Each point in Fig. 3 correspond to an entire community, with on the $x$ axis the average biomass of the community $\langle b^* \rangle$ and on the $y$ axis the average equilibrium production of the community $\langle b^* \; g(b^*) \rangle$. Within each community type the points follow a scaling law with exponent aroun 3/4.

## 6.1 Analytical prediction of average equilibrium production

In order to compute how the average production changes with respect to the average biomass density in our context we can resosrt to the cavity solution computed in the previous section which *mutatis mutandis* in terms of biomass density reads

$$b^* = \left( \frac{\mu S \langle b^* \rangle + \sigma \sqrt{S \langle (b^*)^2 \rangle} \eta}{r \; b_0^{1-k}} \right)^{1/(k-1)} . \tag{59}$$

At equilibrium we have

$$b^* g(b^*) \equiv \underbrace{r b^* \left( \frac{b^*}{b_0} \right)^{k-1}}_{\text{Production}} = \underbrace{b^* (\mu S \langle b^* \rangle + \sigma \sqrt{S \langle (b^*)^2 \rangle} \eta)}_{\text{Losses}} , \tag{60}$$

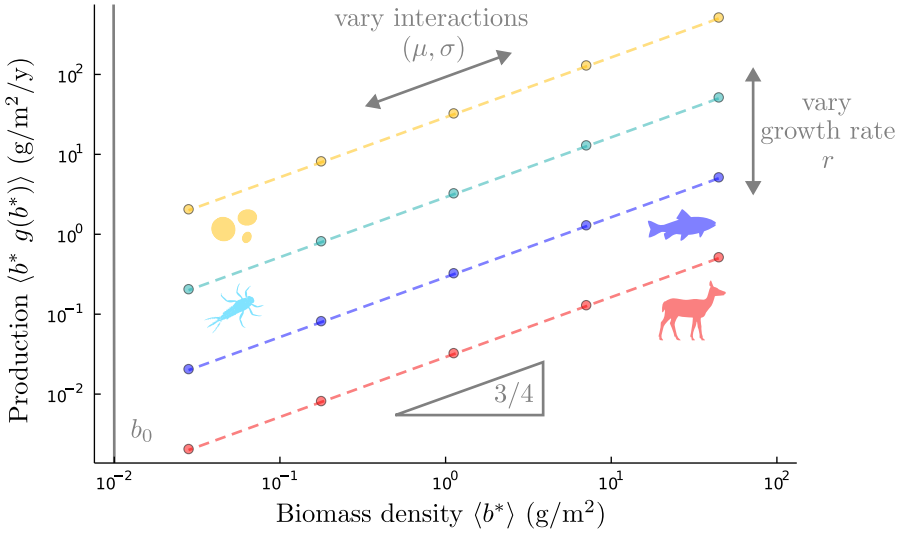


Figure 3: Make figure with precise values of r Average equilibrium production $\langle b^* \; g(b^*)\rangle$ plotted versus average equilibrium biomass density $\langle b^*\rangle$. Each dot represents simulations for a community of $S = 50$ species, each color correspond to a specific growth rate value: $r = 10^2$ yellow, $r = 10$ light blue, $r = 1$ blue and $r = 10^{-1}$ red with the dimension of 1/y. The exponent in the growht rate is set as $k = 3/4$ and the biomass scale is $b_0 = 10^{-2}$ (g/m$^2$), the different points within a color (i.e. same $r$) correspond to $\mu S \in \{r10^2, r10, r, r^1 0^{-1}, r10^{-2}\}$. We set everywhere the coefficient of variation $\sigma/\mu = 0.7$. The dashed lines represent theoretical predictions from the cavity solution.

therefore

$$\langle b^* g(b^*)\rangle = \mu S \langle b^*\rangle^2 + \sigma\sqrt{S\langle (b^*)^2\rangle}\langle b^*\eta\rangle \,. \tag{61}$$

Invoking the gaussian approximation we know that the average reads

$$\langle b^*\rangle = \left(\frac{\mu S}{r \; b_0^{1-k}}\right)^{1/(k-2)} , \tag{62}$$

which, if inverted for $\mu S$, gives

$$\mu S = r \; b_0^{1-k} \langle b^*\rangle^{k-2} \,, \tag{63}$$

which imply that the first term on the r.h.s. of Eq. (61) is equal to $r \; b_0^{1-k}\langle b^*\rangle^k$.

The second term is more involved. By writing explicitely the expression for $b^*$ it reads

$$\begin{aligned}\sigma\sqrt{S\langle (b^*)^2\rangle}\langle b^*\eta\rangle &= \sigma\sqrt{S\langle (b^*)^2\rangle}\left\langle \left(\frac{\mu S\langle b^*\rangle + \sigma\sqrt{S\langle (b^*)^2\rangle}\eta}{r \; b_0^{1-k}}\right)^{1/(k-1)} \eta \right\rangle , \\ &= \sigma\sqrt{S\langle (b^*)^2\rangle} r^{1/(1-k)} b_0 \left\langle \frac{\eta}{(\mu S\langle b^*\rangle + \sigma\sqrt{S\langle (b^*)^2\rangle}\eta)^{1/(1-k)}} \right\rangle . \end{aligned} \tag{64}$$

The leading term in the denominator for large $S$ is $(\mu S\langle b^*\rangle)^{1/(1-k)}$, which for $k = 3/4$ is proportional to $S^4$, while the others have a lower order dependence on $S$. Therefore if we approximate the whole denominator by $(\mu S\langle b^*\rangle)^{1/(1-k)}$ and recall that $\langle\eta\rangle = 0$ we can neglect this term and approximate the average production as

$$\langle b^* g(b^*)\rangle \simeq r \; b_0^{1-k}\langle b^*\rangle^k \,. \tag{65}$$

## 6.2 Note on the origin of sublinear growth

Mechanistic justifications of the emergence of sublinear dynamical growth at the coarse level of description of the model studied in this work should be sought after. However our results suggest that mechanistic descriptions of community dynamics leading to an effective sublinear growth (or, more generally, to a relative change of production with respect of population abundance lower than the relative change of losses, see Sec. 1) will be qualitatively characterized by a positive correlation beteween stability and complexity.

The macroecological data which inspired the model studied in this work have mixed origin, some can be directely connected with dynamical production and other are cross-ecosystem patterns. More precise and systematic observations of the former and validation of the latter at the ecosystem level with temporal data are needed (see Ref. [10] for an example of a macroecologially motivated model and subsequent discussion about within ecosystem validation).

**Among the task that future theoretical work should aim at, we suggest**

- Building a mechanistic understanding of the emergence of sublinear dynamical scaling from realistic models.
- Connecting the abundance prediction from community models with macroecological patterns related to abundance. In particular when we go from within community description to cross-community.
- Exploring in detail possibilities different from sublinear dynamical scaling to explain cross-ecosystem sublinear scaling and test indipendent predicrtions.

**Future urgent experimental and field research include**

- Collecting temporal data within ecosystems and devise ways to estimate the population abundance or density dependence on production.
- Extending the spectrum of data available in order to further validate the evidence of sublinear production.

# 7 Macroecological laws

In this section we compare macroecological patterns with prediction of our model specifying in which way we construct the observable to compare and under which assumptions in addtion to the ones described in the construction of the model.

## 7.1 Species abundance distribution

The species abundance distribution distribution within a community is often well fitted by a log-normal distribution. In order to recover this pattern for the abundance density $n_i$ with our model we assume that the growth rates $r_i$ follows a log-normal distribution.

**Assumptions**

- $\ln r \sim \mathcal{N}(\mu_r, \sigma_r)$.

**Predictions**

- We predict that $n^*$ roughly follows a log-normal distribution as well and, if we consider $k = 3/4$, it has shape parameter 4 times larger than the one for $r$.

We can work out an exact calculation in the case of uniform interactions (i.e. $\sigma \to 0$), which works well also for small but finite $\sigma$. In this case the cavity solution for $n^*$ (Eq. (23)) reads

$$n^* = \left( \frac{\mu S \langle n^* \rangle}{r \; n_0^{1-k}} \right)^{1/(k-1)} , \tag{66}$$

where we recall that consider for simplicity that the scale $n_0$ is the same for all the species in the community and set it to unity, $n_0 = 1$, in the following.

We can obtain the probability distribution for $n^*$ by pushing forward the one for $r$, $P(n^*) = P(r(n^*))|dr/dn^*|$. Given that $r(n^*)$ reads

$$r = \frac{(n^*)^{k-1}}{\mu S \langle n^* \rangle} , \tag{67}$$

and

$$\left| \frac{dr}{dn^*} \right| = \frac{(1-k)(n^*)^{k-2}}{\mu S \langle n^* \rangle} , \tag{68}$$

we obtain that $n^*$ is as well a log-normal random variable

$$\ln n^* \sim \mathcal{N}(\mu_{n^*}, \sigma_{n^*}) , \tag{69}$$

with

$$\mu_{n^*} = \frac{\mu_r - \ln(\mu S \langle n^* \rangle)}{(1-k)} , \tag{70}$$

$$\sigma_{n^*} = \frac{\sigma_r}{(1-k)} . \tag{71}$$

Notice that the scale parameter is amplified by a factor $1/(1-k)$, which in the case of $k \simeq 3/4$ correspond to a species abundance distribution four times wider than the growth rate distribution.

In this case we only need to solve a self-consistent equation for the average $\langle n^* \rangle$ to complete the cavity solution. This can be done analytically because the expression of the average for a log-normal distribution is known

$$\langle n^* \rangle = \exp\left( \mu_{n^*} + \frac{\sigma_{n^*}^2}{2} \right) , \tag{72}$$

and we have

$$\langle n^* \rangle = (\mu S)^{(k-2)} \exp\left[ \frac{2\mu_r(1-k) + \sigma_r^2}{2(1-k)(2-k)} \right] . \tag{73}$$

In Fig. 4 the cavity results are compared with simulations showing perfect agreement in the case $\sigma \to 0$ (left panel) and good agreement also in the case of finite $\sigma$ (right panel).

In Fig. 5 we report the abundance distributions for the four community types as parametrized in the model construction (details in caption).

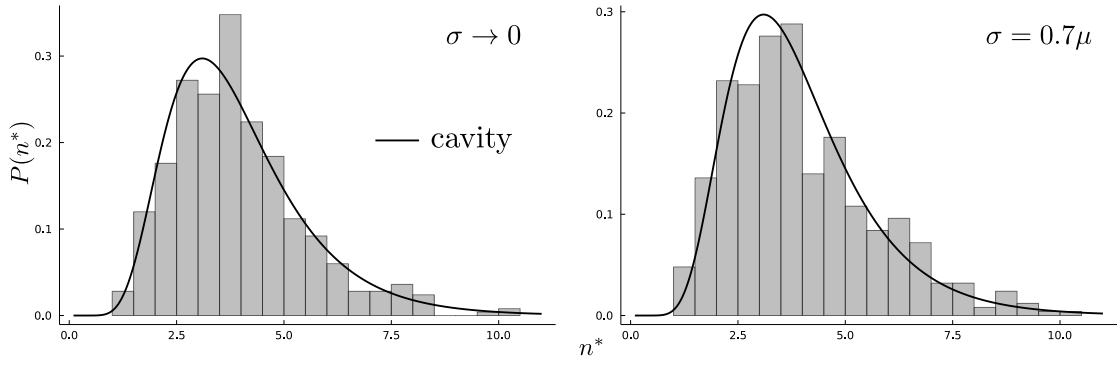


Figure 4: Cavity solution compared to simulations for log-normal distribution of growth rates $r$, $\ln P(r) = \mathcal{N}(\mu_r, \sigma_r)$, with $\mu_r = 1$ and $\sigma_r = 1/10$ and a pool of $S = 500$ species with $\mu = 10^{-3}$, $k = 3/4$ and $\sigma \to 0$ (left panel) while $\sigma = 0.7\mu$ (right panel).

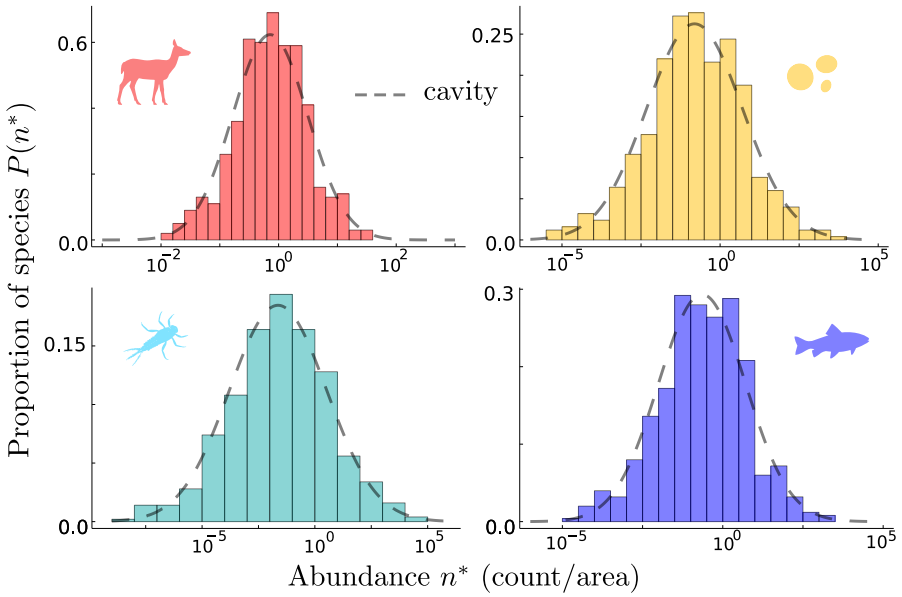


Figure 5: Abundance distribution of species resulting from the dynamics for the four community types as parametrized in the model construction see (Fig. 3), but with $S = 500$ species to obtain better statistics. In particular, in every panels, we set $\mu S = \langle r \rangle$ and $\sigma/\mu = 0.7$ and $r$ is lognormally distributed with mode chose as $\exp(\mu_r) = \langle r \rangle B_0^{1-k}$ specific for each color as per model construction and shape parameter $\sigma_r = 0.16$ for red, 0.38 for blue, 0.54 for light blue and 0.34 for yellow. The dashed lines correspond to the cavity solution in Eq. (69) which well compare with simulations.

## 7.2 Mean-variance scaling

The variance of fluctuations in biomass densities for time series of different species scale with mean biomass density with an exponent from 3/2 to 2. We consider again a log-normal distribution for $r$ and that the loss term of our model exhibits variation in mortality (e.g. $\mu$ varies).

**Assumptions**

- $\ln r \sim \mathcal{N}(\mu_r, \sigma_r)$ (only needed for analytical results).
- $\mu$ varies (in the case of uniform $r$, the ratio $\mu/\sigma$ should be constant).

**Predictions**

- Taylor's law.

We consider again the cavity result in the limit $\sigma \to 0$ which, in the case of $\ln r \sim \mathcal{N}(\mu_r, \sigma_r)$, gives $\ln b^* \sim \mathcal{N}(\mu_{b^*}, \sigma_{b^*})$ with

$$\mu_{b^*} = \frac{\mu_r - \ln(\mu S \langle b^* \rangle)}{(1-k)}, \tag{74}$$

$$\sigma_{b^*} = \frac{\sigma_r}{(1-k)}. \tag{75}$$

By varying $\mu$ only the scale parameter $\mu_{b^*}$ is modified. Therefore if we consider the mean and variace of the log-normal distribution

$$\langle b^* \rangle = \exp\left(\mu_{b^*} + \frac{\sigma_{b^*}^2}{2}\right), \tag{76}$$

$$\mathrm{var}(b^*) = \left(\exp[\sigma_{b^*}^2] - 1\right) \exp\left(2\mu_{b^*} + \sigma_{b^*}^2\right), \tag{77}$$

$$\tag{78}$$

it is straightforward to realize that the mean is proportional to $\exp(\mu_{b^*})$, while the variance to $\exp(2\mu_{b^*})$, therefore

$$\mathrm{var}(b^*) \propto \langle b^* \rangle^2, \tag{79}$$

i.e., Taylor's law. In Fig. 6 we report a comparison with simulations with lognormally distributed $r$ and $\sigma \to 0$, lognormally distribute $r$ and finite $\sigma = \mu/10$, to show that the results hold in this case, and, even if in this case we don't have analytical results (I manage to obtain one, to be added), also with uniform $r = 1$ and finite $\sigma = \mu/10$.

In Fig. 7 we report variance vs. average for the communitites parametrized as in model construction (Fig. 3), finding a good agreement with Taylor's law, see caption for details.

## 7.3 Size-density scaling

The species-level relation of population density vs. body mass is nearly inversely proportional across major groups. By relying on no further assumptions then in those used to connect the model with data on production we predict a size-density scaling with exponent -1.

**Assumptions**

- Same as for the connection of the model with data on production.

**Predictions**

- Size-density scaling with exponent -1.

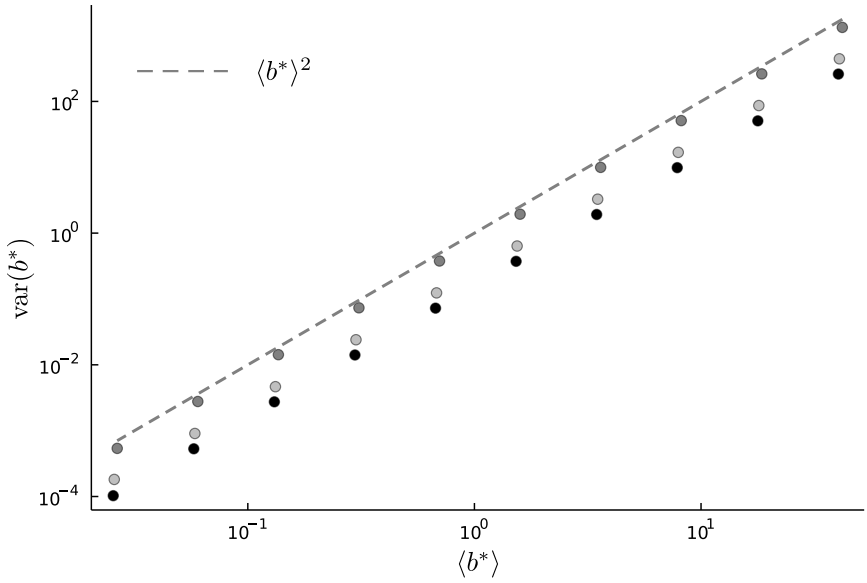


Figure 6: Variance of the species biomass density distribution plotted against the mean, each dot is a community with a specific $\mu \in \{\langle r \rangle 10^{-2}, \langle r \rangle 10^2\}$, whith $S = 10^3$, $k = 3/4$ and black dots correspond to $\ln P(r) = \mathcal{N}(\mu_r, \sigma_r)$, with $\mu_r = 1$, $\sigma_r = 1/10$ and $\sigma \to 0$, dark gray to $\sigma = \mu/10$ with the same distribution for $r$ and light gray dots correspond to uniform $r = 1$ and $\sigma = \mu/10$.

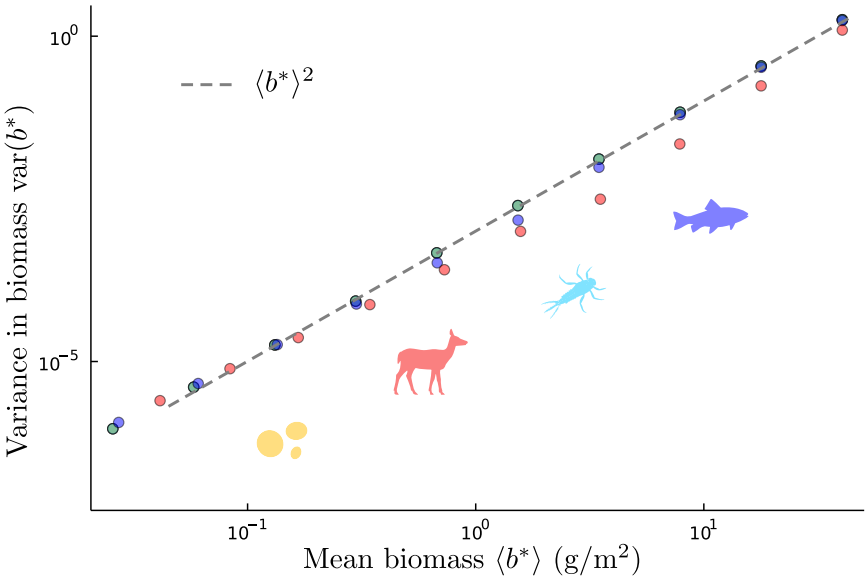


Figure 7: Make figure with precise values of r Variance of the species biomass density distribution plotted against the mean, each dot is a community is parametrized as in the model construction (see caption of Fig. 3).

We start from the cavity solution for the equilibrium biomass density $b_0$

$$b^* = \left( \frac{\mu S \langle b^* \rangle + \sigma \sqrt{S \langle (b^*)^2 \rangle \eta}}{r \; b_0^{1-k}} \right)^{1/(k-1)} , \tag{80}$$

where we consider $r$ uniform and different for each community type as in the model connection with data on production. Each community is characterized by an average mass $m$, and, given that we consider $\mu S \propto r$ (it varies in a range of two order of magnitude above and below $r$), it cancels out with $r$ leaving no mass dependence. Therefore the average numerical densities $\langle n^* \rangle$ of different community types will be inversely proportional to their mass $m$ with a spread on the $y$ axes due to different $(\mu, \sigma)$

$$\langle n^* \rangle \sim m^{-1} . \tag{81}$$

In Fig. 8 we report the average numerical density vs. body mass for the different community types using the same parameters from Fig. 3.

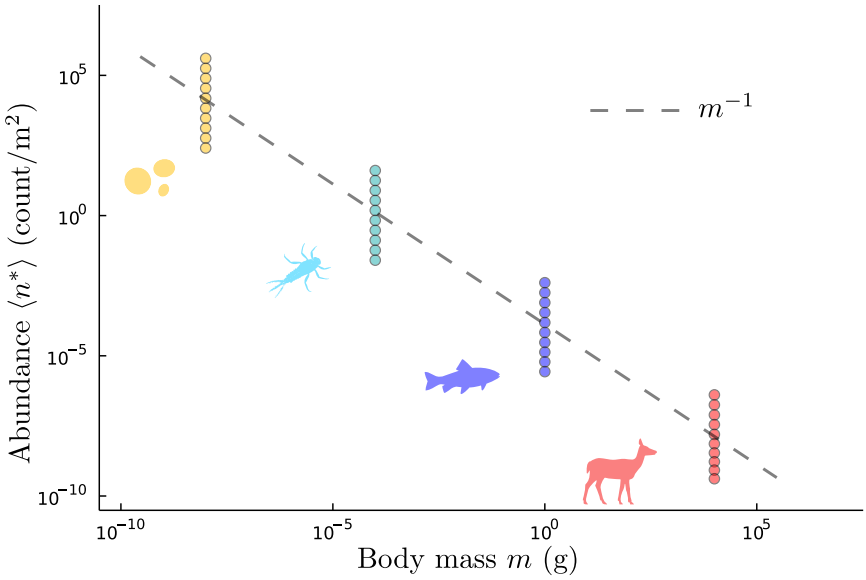


Figure 8: Make figure with precise values of r Numerical density distribution vs. body mass for each community type parametrized as in the model construction (Fig. 3).

# 8 Back up sections

## 8.1 Generalized Lotka-Volterra with generic production

Maybe take out.

Consider a competitive community of $S$ species defined by the following dynamics for the population abundances

$$\frac{dx_i}{dt} = g(x_i) - x_i \sum_{j \neq i} A_{ij} x_j \,, \tag{82}$$

where the $A_{ij}$ are extracted from a distribution with mean $\mu > 0$ and standard deviation $\sigma$ and the production term $g_i(x_i)$ may in principle include self-regulation terms which are only dependent on species $i$ and parameters typical of species $i$.

If the equilibrium is feasible, denoting $x_i^*$ the equilibrium values, we have

$$g_i(x_i^*) = x_i^* \sum_{j \neq i} A_{ij} x_j^* \,. \tag{83}$$

The jacobian evaluated at equilibrium is formally

$$J_{ij}\Big|_{\mathbf{x}=\mathbf{x}^*} = -x_i^* A_{ij} \,, \tag{84}$$

$$J_{ii}\Big|_{\mathbf{x}=\mathbf{x}^*} = g_i'(x_i^*) - \frac{g_i(x_i^*)}{x_i^*} \,, \tag{85}$$

where $g_i'(x_i^*)$ stands for $|dg_i(x_i)/dx_i|_{x_i=x_i^*}$ and we used the equilibrium relation.

In order to make some analytical progress let us focus on the case of uniform interactions ($\sigma \to 0$) and production with same parameters for every species, i.e. $g_i = g \ \forall i$. Then every species have the same equilibrium value $x_i^* = x^* \ \forall i$ and we can write down the equilibrium relation

$$g(x^*) = (S-1)\mu (x^*)^2 \,, \tag{86}$$

and the jacobian at equilibrium

$$J_{ij}\Big|_{x=x^*} = -x^* \mu \,, \tag{87}$$

$$J_{ii}\Big|_{x=x^*} = g'(x^*) - \frac{g(x^*)}{x^*} \,. \tag{88}$$

The largest eigenvalue correspond to

$$\lambda_{\max} = J_{ii}\Big|_{x=x^*} - J_{ij}\Big|_{x=x^*} \,, \tag{89}$$

therefore the stability condition reads

$$g'(x^*) - \frac{g(x^*)}{x^*} + x^* \mu < 0 \,. \tag{90}$$

By exploiting the equilibrium relation we can recast the last inequality as

$$g'(x^*) - \frac{g(x^*)}{x^*} + \frac{g(x^*)}{x^*(S-1)} < 0 \,, \tag{91}$$

therefore giving the general formal stability condition in terms of production at equilibrium and equilibrium density

$$g'(x^*) < \frac{g(x^*)}{x^*}\left(1 - \frac{1}{S-1}\right), \tag{92}$$

which for $S \to \infty$ can be approximated by

$$g'(x^*) < \frac{g(x^*)}{x^*}. \tag{93}$$

This last stability condition is quite general and, exploiting the trivial identity $1 = dx/dx|_{x=x^*} =: (x^*)'$, it can be written as

$$\frac{g'(x^*)}{g(x^*)} < \frac{(x^*)'}{x^*}, \tag{94}$$

which means that the relative change in growth should be less than the relative change in abundance itself.

Logistic and sublinear cases are recovered by substitutig resepctively $g(x) = x(1 - x/K)$ and $g(x) = x^k$.

## References


[1] Guy Bunin. Ecological communities with Lotka-Volterra dynamics. *Physical Review E*, 95(4):042414, apr 2017.

[2] Matthieu Barbier, Jean-François Arnoldi, Guy Bunin, and Michel Loreau. Generic assembly patterns in complex ecological communities. *Proceedings of the National Academy of Sciences*, 115(9):2156–2161, 2018.

[3] Matthieu Barbier and Jean-François Arnoldi. The cavity method for community ecology. *bioRxiv*, 2017.

[4] Madhu Advani, Guy Bunin, and Pankaj Mehta. Statistical physics of community ecology: a cavity solution to MacArthur's consumer resource model. *Journal of Statistical Mechanics: Theory and Experiment*, 2018(3):033406, mar 2018.

[5] Wenping Cui, Robert Marsland Iii, and Pankaj Mehta. Effect of Resource Dynamics on Species Packing in Diverse Ecosystems. *Physical Review Letters*, 125, 2020.

[6] Satya N. Majumdar, Arnab Pal, and Grégory Schehr. Extreme value statistics of correlated random variables: A pedagogical review. *Physics Reports*, 840:1–32, jan 2020.

[7] F. Roy, G. Biroli, G. Bunin, and C. Cammarota. Numerical implementation of dynamical mean field theory for disordered systems: application to the Lotka–Volterra model of ecosystems. *Journal of Physics A: Mathematical and Theoretical*, 52(48):484001, nov 2019.

[8] Yashar Ahmadian, Francesco Fumarola, and Kenneth D. Miller. Properties of networks with partially structured and partially random connectivity. *Physical Review E - Statistical, Nonlinear, and Soft Matter Physics*, 91(1):012820, jan 2015.

[9] Ian A. Hatton, Andy P. Dobson, David Storch, Eric D. Galbraith, and Michel Loreau. Linking scaling laws across eukaryotes. *Proceedings of the National Academy of Sciences of the United States of America*, 116(43):21616–21622, oct 2019.

[10] Matthieu Barbier, Laurie Wojcik, and Michel Loreau. A macro-ecological approach to predation density-dependence. *Oikos*, 130(4):553–570, apr 2021.